HHS Public Access

Author manuscript

IEEE J Sel Top Quantum Electron. Author manuscript; available in PMC 2017 May 01.

Published in final edited form as:

IEEE J Sel Top Quantum Electron. 2016 ; 22(3): . doi:10.1109/JSTQE.2016.2524618.

Acoustic Radiation Force Optical Coherence Elastography of Corneal Tissue

Yueqiao Qu[*],
Department of Biomedical Engineering, the Edwards Life Sciences Center for Advanced Cardiovascular Technology, and Beckman Laser Institute, University of California, Irvine, Irvine, CA 92697 USA

Teng Ma[*],
NIH Ultrasonic Transducer Resource Center and the Department of Biomedical Engineering, University of Southern California, Los Angeles, CA, USA

Youmin He,
Beckman Laser Institute, University of California, Irvine, Irvine, CA 92612 USA

Jiang Zhu,
Beckman Laser Institute, University of California, Irvine, Irvine, CA 92612 USA

Cuixia Dai,
Beckman Laser Institute, University of California, Irvine, Irvine, CA 92612 USA, and the Shanghai Institute of Technology, 100 Haiquan Road, Fengxian, Shanghai, China

Mingyue Yu,
NIH Ultrasonic Transducer Resource Center and the Department of Biomedical Engineering, University of Southern California, Los Angeles, CA, USA

Shenghai Huang,
Beckman Laser Institute, University of California, Irvine, Irvine 92612 USA and the School of Ophthalmology and Optometry, Wenzhou Medical University, Wenzhou, 325027 China

Fan Lu,
School of Ophthalmology and Optometry, Wenzhou Medical University, Wenzhou, 325027 China

K. Kirk Shung [Life Fellow, IEEE],
NIH Ultrasonic Transducer Resource Center and the Department of Biomedical Engineering, University of Southern California, Los Angeles, CA, USA

Qifa Zhou [Senior Member, IEEE], and
NIH Ultrasonic Transducer Resource Center and the Department of Biomedical Engineering, University of Southern California, Los Angeles, CA, USA

Zhongping Chen

Please address all correspondence to Dr. Q. Zhou and Dr. Z. Chen
[*]First two authors contributed equally to this work
Y. Qu and T. Ma have equal contributions and are treated as co-first authors.

Dr. Z. Chen has a financial interest in OCT Medical Imaging Inc., which, however, did not support this work.

Department of Biomedical Engineering, the Edwards Life Sciences Center for Advanced Cardiovascular Technology, and Beckman Laser Institute, University of California, Irvine, Irvine, CA 92697 USA

Yueqiao Qu: yueqiaoq@uci.edu; Teng Ma: tengma@usc.edu; Youmin He: youminhe@gmail.com; Jiang Zhu: jzhumail@gmail.com; Cuixia Dai: sdadai7412@163.com; Mingyue Yu: mingyue930@gmail.com; Shenghai Huang: youtu8@gmail.com; Fan Lu: lufan@mail.eye.ac.cn; K. Kirk Shung: kkshung@usc.edu; Qifa Zhou: qifazhou@usc.edu; Zhongping Chen: z2chen@uci.edu

Abstract

We report on a real-time acoustic radiation force optical coherence elastography (ARF-OCE) system to map the relative elasticity of corneal tissue. A modulated ARF is used as excitation to vibrate the cornea while OCE serves as detection of tissue response. To show feasibility of detecting mechanical contrast using this method, we performed tissue-equivalent agarose phantom studies with inclusions of a different stiffness. We obtained 3-D elastograms of a healthy cornea and a highly cross-linked cornea. Finally we induced a stiffness change on a small portion of a cornea and observed the differences in displacement.

Index Terms

OCT; elastography; ARF; cornea

I. Introduction

The cornea is primarily composed of cross-linked collagen fibers, which provides it with high tensile strength and serves as a protective coat to the eye [1]. It is an essential portion in the refraction of light entering the eye, and when there is a disruption in the collagen fiber network, such as in the case of keratoconus, corneal refractive function is compromised, affecting vision [2]. Keratoconus is a disease characterized by changes in the cross-linking properties, high corneal curvature, reduced corneal thickness, and tissue topographic irregularity [3]. In addition to natural diseases, refractive surgeries such as LASIK alter biomechanical properties of the cornea, resulting in conditions such as progressive post-LASIK keratectasia (PPLK) [4]. PPLK is a progressive deformation of the cornea that occurs within two years of surgery, causing disruptions in the collagen cross-linking network [4–5]. In both PPLK and keratoconus, a common management solution is corneal collagen crosslinking treatment, which allows for biomechanical stability of the cornea by increasing the intra- and interfibrillar rigidity [5]. With the increasing popularity of refractive surgeries, as well as the natural occurrences of corneal diseases, there is an increasing need for understanding the biomechanical properties of ocular tissue for diagnosis and progression tracking.

The ocular response analyzer (ORA) has been used to measure the mechanical properties of the cornea. It analyzes the response of ocular tissue to an air pressure, focusing on the hysteresis of the relaxation [6]. However, factors such as the corneal thickness and curvature are not accounted for in ORA. The Corvis tonometer is another technology that visualizes and measures the deformation of the cornea in response to an air impulse [7]. However, the response measurements are taken for the entire cornea as a whole, and cannot focus on a

small region of interest. This is problematic in diagnosing ocular diseases in their early stages. In the last decade, elastography methods have been used to analyze localized biomechanical properties of tissues in clinics [8–9].

Several acoustic radiation force (ARF)-based ultrasound elastography techniques by using low frequency excitation and high frequency detection methods have been developed to characterize the mechanical properties of tissues, such as the cornea and coronary artery [10,11]. However, ultrasonic elastography is still limited in resolution and is not ideal for detecting small biomechanical changes. Optical coherence elastography (OCE), which utilizes optical methods and has micron-scale resolution, has gained momentum in characterizing subtle changes in tissue mechanical properties during the early stages of diseases [12]. Recently, ultrafast OCE methods have been used to obtain both 2D and 3D volumetric data quickly, and are rapidly progressing toward translational research [13–14]. These methods use air puff or compression techniques for tissue excitation. In the case of the air puff technique, full quantification of a depth resolved corneal image requires measurement and modeling of the shear wave across the entire cornea, which may have limitations when working with diseased corneas where lateral changes play an important role. Compression OCE is highly contact-based and not ideal for translation and *in vivo* studies. OCE has also been performed on corneal tissue by analyzing the propagation of shear waves [15–17]. However, these corneal imaging methods do not currently offer real-time imaging of the elasticity map.

We have recently reported on an OCE method using ARF as dynamic excitation to obtain high-speed, high-resolution elastogram mapping of tissues [18–120]. In this method, we apply a modulated square wave acoustic force to the sample and detect the phase shifts of the sample oscillation using phase-resolved optical coherence tomography (OCT) [18–121]. Phase resolved OCT is a noncontact method to track the compression waves and thus the tissue elasticity within the 3D imaging region. In this paper, we validate the ARF-OCE system detection of axial and lateral changes in mechanical stiffness. We also use the imaging system for healthy corneal tissue as well as tissue with induced corneal sclerosis to compare the resulting Young's modulus.

II. ARF-OCE System Validation

A. System Set-up

The OCE system uses an ultrasonic transducer system for excitation of the sample, phase-resolved OCT system for detection of the vibrational response, and a computer for image processing. The schematic diagram is shown in Fig. 1. The axial resolution of the system is 2.5 μm while the lateral resolution is 15 μm. A function generator feeds a square wave modulated signal into an amplifier, which generates an acoustic radiation force via a focused ring transducer of 4.5 MHz. The ultrasound transducer has a uniform stress field within approximately a 400 um by 400 um lateral region, with a larger axial field of 5 mm. The optical system is based on a superluminescent diode source with a central wavelength of 890 nm, and a bandwidth of 150 nm. The light traveling to the sample and reference arms splits in an 80/20 coupler. The light from the reference is delayed and reflected back with a mirror. The light in the sample arm goes through the hollow ring in the middle of the transducer and

interacts with the phantom or tissue in the focal zone, which overlaps with the acoustic zone of the transducer to generate a strong phase signal. The power from the sample arm is measured to be 0.89 mW, which is below the safe value determined by the American National Institute (ANSI).

The light then travels back into the camera arm, which houses a collimator, a diffraction grating, a focusing lens, and a CMOS camera for detection of the interference signal. A line scan CMOS detector, which can operate at up to 70k A-lines per second, is used in place of the CCD camera in the previous manuscripts for faster imaging. However, in these *ex-vivo* experiments, an A-line rate of 20kHz is used to capture OCT images and the OCE oscillations.

B. Transducer Characterization

The acoustic profiles of the ultrasonic excitation transducer and OCT scanning beam were arranged in a confocal configuration on the same side of the imaging sample under the guidance of a hydrophone. The normalized pressure profile of the transducer is shown in figure 2. The region of uniform pressure is small in the lateral direction at the axial focus as shown in figure 2a and the axial beam profile is shown in 2b.. The relationship between the ARF and the intensity, I, distribution is summarized as $F=2\alpha \mathbf{I}/\mathbf{c}$, where α represents the absorption coefficient and c is the longitudinal wave speed [22]. During imaging, the transducer was pulled away from the focal region in the axial direction in order to achieve a uniform stress region of approximately 600 um. Last, Doppler methods are used to determine the phase shifts between A-lines, where a larger phase change corresponds to high displacement and a softer sample. There is high phase stability of a few milliradians for a spectral domain OCT system [18].

C. Phantom Imaging

We had previously verified the lateral contrast of ARF-OCE imaging using a two-sided phantom [15–17], but it is still necessary to show feasibility for axial contrast. An agarose tissue-mimicking phantom with a stiffer inclusion was fabricated. The stiff inclusion has a diameter of about 1 mm, consisting of 0.8% agarose (by weight). It is buried within the larger phantom of 0.3% agarose. The completed sample, which is round with a diameter of 3.5 cm and a thickness of 1 cm, was placed on a holder for OCE imaging.

To determine the feasibility of this agarose phantom, we calculated the displacements of two uniform samples under different excitation voltages shown in Fig. 3a. A linear dependency of the ultrasound-induced displacement on the excitation voltage was found, and a 500 mVpp excitation voltage was used for the rest of this study.

The OCT and OCE displacement images of the inclusion phantom are shown in Figs. 3b and 3c, respectively. The boundary between the two phantoms is evident in the OCT image likely because of water at the interface when the phantom was made, which contributes to a high scattering signal. In the OCE image, the boundary of the two phantoms is evident because of the differences in vibrational response. The shape of the two phantoms is clearly

distinguishable from the OCE image in all directions, which proves that our system is able to detect differences in the mechanical properties of tissue both laterally and axially.

Mechanical Testing vs. Experimental Results—Using the phase change, represented by Δφ(z,t), and the Doppler relationship, it is possible to extract the velocity, v, of the phantom oscillation as shown in equation 1. The displacement can be calculated using the velocity measurements and integrating over time, also depicted in equation 1. λ_0 is the central wavelength, n is the refractive index, τ is the 50 us exposure time, and θ is the Doppler angle. The mean displacement ratio of the softer phantom to the stiffer inclusion is approximately 3.49 : 1 according to the experimental results in figure 3. The Young's Modulus of a material is defined in equation 2, where σ is the stress, d is displacement, and z is axial depth. In this way, the stiffness of a sample varies inversely with its induced displacement values, and relative stiffness can be obtained if the displacement is calculated. The relative stiffness of the surrounding phantom to the rod inclusion of the agarose phantom is 1: 3.49.

$$\Delta d = \int v dt = \int \frac{\Delta\phi(z,t)\lambda_0}{4\pi n\tau \cos\theta} dt \quad \text{[Equation 1]}$$

$$Y = \frac{\sigma}{\Delta d / z} \quad \text{[Equation 2]}$$

Compression tests were performed using MTS Synergie 100 on both the 0.3% and a 0.8% agarose phantom, with resulting Young's Moduli of 3.68 kPa and 12.24 kPa, respectively. This corresponds to a stiffness ratio of 1: 3.33, which is in close agreement with our experimental result of 1: 3.49.. A strain of up to 0.1 mm/mm with a strain rate of 50 mm/min was used for testing. The feasibility of the ARF-OCE system to detect relative axial and lateral contrast in mechanical properties is shown.

III. Imaging of Corneal Tissue

A. Cross-linking Over 12 Hours

To test the feasibility of our imaging system on corneal tissues, we collected fresh rabbit eyeballs and obtained 3-D images of the rabbit cornea. All experiments were performed within 24 hours of eyeball extraction to ensure freshness. First, the healthy eyeball was placed inside a holder and covered with optically clear gel to hold the sample in place during excitation. A 3 mm by 3 mm area was scanned in the center of the cornea by using OCT, as shown in the 3-D reconstruction in Fig. 4a. OCE imaging was performed within a smaller area with a 400 Hz ARF modulation frequency. The 3-D OCE images were reconstructed and shown in Fig. 4b, with the color representing the phase shift of the tissue with respect to adjacent A-lines.

We also aimed to change the stiffness of the corneal tissue by inducing cross-linking using formalin solution. The entire eyeball was removed from the system and soaked with droplets

of 10% formalin solution. After soaking for 12 hours, we placed the sample back into the system to observe the changes. We assume that after 12 hours, the formalin-induced crosslinking is uniform in the entire cornea, and 3D OCE was performed on a small region using the same ultrasonic excitation conditions. The results are shown in Fig. 4c, where it was apparent that the phase shift has decreased drastically. The displacement amplitude ratio of the healthy cornea to the formalin soaked one was calculated to be 6.34 ± 0.22: 1.

Since the cornea was soaked for 12 hours, it was speculated that the mechanical changes could have been influenced by other factors, such as changes in the freshness of the cornea or instabilities of the system with change in time. In addition, the difference in stiffness changed over 6 fold in this case, which makes it easy to detect.

B. Instantaneous Cross-linking

In order to induce a stiffness change within a single cornea to eliminate other factors affecting the system and simultaneously image tissue of different stiffness, we injected 0.01 ml of 10% formalin inside the healthy cornea via a 1-cc disposable syringe with a 30-gauge needle. The cornea was allowed to sit for merely ten minutes while we prepared for the imaging and zoomed into the area of injection. As shown in Fig. 5a, the OCT image reveals that the left side, where the formalin solution was injected, is distinctly thicker than the right due to the formalin bubble. The tissue was excited with a 400 Hz modulation frequency and a 500 mVpp pre-amplified voltage given to the transducer. The OCE displacement magnitude image is shown in Fig. 5b, with a red color representing high displacement. A much smaller displacement shift is shown on the left side, where the injection took place. Both OCT and OCE images were averaged over 50 B-scans for better representation. The displacement shifts of the raw OCE images before magnitude extraction are shown in Fig. 5c, which corresponds to a smaller displacement on the left side that vibrates much less than the right. The displacement ratio of the healthy side on the right to the cross-linked portion on the left is approximately 1.82 ± 0.04: 1. There is a gradient in the middle portion of the image, similar to that of the phantom studies in Fig. 3. Over time, the formalin solution would diffuse across the entire cornea and the OCE image would resemble that in Fig. 4c. It was noticed that the displacement ratio of 1.82 ± 0.04 was much smaller. It is likely because we did not soak the cornea for nearly as long, so less cross-linking took place within the tissue. It is also important to note that the displacement values begin to decrease on the right side of the image, which is where the uniform acoustic focal zone ends at approximately 600 um.

IV. Discussion and Conclusion

We have demonstrated the feasibility of using an ARF-OCE system for assessing the mechanical properties of corneal tissue. The feasibility of the imaging system to detect mechanical contrast both laterally and axially was tested on an inclusion dual-layered agarose phantom with a difference in stiffness in the two layers of 3.33 fold. The experimental Young's moduli ratios corresponded well with the mechanical compression test results under acoustic radiation forces. We have performed *in vitro* imaging of a healthy rabbit cornea as well as a cross-linked one. The OCT image changed little, but the OCE

showed a 6-fold change. Last, we induced tissue cross-linking on a small area within the same cornea, and observed an approximately 2-fold difference in the stiffness.

These results show that our ARF-OCE method has great potential in distinguishing diseased corneal tissue from normal ones and quantitatively characterizing the severity of the change in mechanical properties. However, there are still a few limiting factors that must be improved before this system can be used for diagnosis purposes.

First, the intraocular pressure (IOP) of the cornea may have been altered during the injection of formalin. In addition, cross-linking may also have had an effect on the IOP, which in turn affected the stiffness measurements. This makes it difficult to distinguish between the changes in stiffness caused by the IOP versus tissue properties when we image different cornea samples. However, when we are looking at relative elasticity from a single sample with the same IOP, the relative values for a single cornea in figure 5 would not be changed by the overall IOP change.

Second, the imaging area must be increased to accommodate the entire cornea. Currently the uniform stress field occurs within a 400 um window, (600 um with pullback away from the focal plane), which is not enough to image an entire rabbit cornea. The rabbit cornea, which is typically approximately 14 mm in diameter, with a center of 6 mm. The first solution would be to increase this coverage by pulling away from the focal region and inducing a larger ARF while compromising the sensitivity. Another alternative would be to perform mechanical scanning over the entire tissue sample to cover more area without changing the force. This method compromises the imaging time. Therefore, it is necessary to find the balance between the two solutions and optimize the system for ocular imaging.

Third, we have not yet considered the effects of the non-uniform ARF in the axial direction, which explains why small changes within corneal layers were not detected. In future studies, we will do calibration studies and increase the sensitivity of our system.

Next, the mechanical index (MI) for ocular applications is 0.23 as determined by the FDA. Based on our results, the MI for the ARF is 1.68. The thermal index (TI) is 1.7 degrees for a scan. Current ARF induced displacement is on the order of micrometer, which is similar to that of ultrasound. Since OCE has nanometer-resolution, it is possible to achieve a sensitivity that is 100 times higher than elastography based on ultrasound. This means that it is possible to decrease power by at least a factor of 10 and still be sensitive enough to observe mechanical contrast. For this preliminary study, we are aiming to test the feasibility of using this technology on the characterization of corneal tissue, so a relatively large excitation was used. In the future, we will decrease the ARF when working with *in vivo* models so that both indices satisfy FDA rules.

Finally, in order to translate this technique to live human imaging, it would be necessary to work with contact-based probe methods or use ultrasonic coupling gel for the acoustic waves to propagate [22–23]. This may cause some discomfort, and biocompatibility factors must be considered. This is a limitation that we are currently working on as we move to *in vivo* studies.

In conclusion, we reported on corneal imaging using an ARF-OCE system, obtaining both phantom results for validation and *ex vivo* tissue tests. These results validate the feasibility of using this system for relative mechanical elasticity testing and show its capabilities in demonstrating corneal cross-linking. Although a number of challenges remain to translate this technology for clinical applications, this technique has great promise for the characterization and diagnosis of corneal diseases.

Acknowledgments

This work was supported in part by the National Institutes of Health under grants R01 HL-125084, R01 HL-105215, R01 EY-021529, P41 EB-10090, P41 EB-015890, and R01 HL-127271.

References

1. Kotecha A. What Biomechanical Properties of the Cornea Are Relevant for the Clinician? Survey of Ophthalmology. 2007; 52(2):109–114.
2. Ruberti JW, Roy AS, Roberts CJ. Corneal Biomechanics and Biomaterials. The Annual Review of Biomedical Engineering. 2011; 13:269–295.
3. Roy AS, Shetty R, Kummelil MK. Keratoconus: A biomechanical perspective on loss of corneal stiffness. Indian Journal of Ophthalmology. 2013; 61(8):392–393. [PubMed: 23925321]
4. Comaish IF, Lawless MA. Progressive post-LASIK keratectasia: Biomechanical instability or chronic disease process? J. Cataract Refract. Surg. 2002; 28:2206–2213. [PubMed: 12498861]
5. Salgado JP, Khoramnia R, Lohmann CP, Winkler von Mohrenfels C. Corneal collagen crosslinking in post-LASIK keratectasia. Br. J. Ophthalmol. 2010; 10:1–5.
6. Luce DA. Determining in vivo biomechanical properties of the cornea with an ocular response analyzer. J. Cataract Refract. Surg. 2005; 31:156–162. [PubMed: 15721708]
7. Hon Y, Lam AKC. Corneal Deformation Measurement Using Scheimpflug Noncontact Tonometry. Optometry and Vision Science. 2013; 90:e1–e8. [PubMed: 23238261]
8. Sarvazyan A, Hall TJ, Urban MW, Fatemi M, Aglyamov SR, Garra BS. An overview of elastography – an emerging branch of medical imaging. Curr. Med. Imaging Rev. 2011; 7(4):255–282. [PubMed: 22308105]
9. Kennedy BF, Kennedy KM, Sampson DD. Review of Optical Coherence Elastography Fundamentals, Techniques, and Prospects. IEEE Journal of Selected Topics in Quantum Electronics. 2014; 20(2):7101217.
10. Shih C, Huang C, Zhou Q, Shung KK. High-Resolution Acoustic-Radiation-Force-Impulse Imaging for Assessing Corneal Sclerosis. IEEE Transactions on Medical Imaging. 2013; 32(7): 1316–1324. [PubMed: 23584258]
11. Ma T, Qian X, Chiu CT, Yu M, Jung H, Tung YS, Shung KK, Zhou Q. High-resolution harmonic motion imaging (HR-HMI) for tissue biomechanical property characterization. Quantitative imaging in medicine and surgery. 2015; 5:108–117. [PubMed: 25694960]
12. Schmitt JM. OCT elastography: imaging of microscopic deformation and strain of tissue. Optics Express. 1998; 3(6):199–211. [PubMed: 19384362]
13. Singh M, Wu C, Liu C, Li J, Schill A, Nair A, Larin K. Phase-sensitive optical coherence elastography at 1.5 million A-Lines per second. Optics Letters. 2015; 40(11):2588–2591. [PubMed: 26030564]
14. Kennedy B, Malheiro FG, Chin L, Sampson DD. Three-dimensional optical coherence elastography by phase-sensitive comparison of C-scans. Journal of Biomedical Optics. 2014; 19(7):076006. [PubMed: 25003754]
15. Nguyen T, Arnal B, Song S, Huang Z, Wang RK, O'Donnell M. Shear wave elastography using amplitude-modulated acoustic radiation force and phase-sensitive optical coherence tomography. Journal of Biomedical Optics. 2015; 20(1):016001. [PubMed: 25554970]

16. Wang S, Larin KV. Shear wave imaging optical coherence tomography (SWI-OCT) for ocular tissue biomechanics. Optics Letters. 2014; 39(1):41–44. [PubMed: 24365817]
17. Zhu J, Qu Y, Ma T, Li R, Du Y, Huang S, Shung KK, Zhou Q, Chen Z. Imaging and characterizing shear wave and shear modulus under orthogonal acoustic radiation force excitation using OCT Doppler variance method. Optics Letters. 2015; 40(10)
18. Qi W, Chen R, Chou L, Liu G, Zhang J, Zhou Q, Chen Z. Phase-resolved acoustic radiation force optical coherence elastography. Journal of Biomedical Optics. 2012; 17(11):110505. [PubMed: 23123971]
19. Qi W, Li R, Ma T, Li J, Shung KK, Zhou Q, Chen Z. Resonant acoustic radiation force optical coherence elastography. Applied Physics Letters. 2013; 103:103704. [PubMed: 24086090]
20. Qi W, Li R, Ma T, Shung KK, Zhou Q, Chen Z. Confocal acoustic radiation force optical coherence elastography using a ring ultrasonic transducer. Applied Physics Letters. 2014; 104(12): 123702. [PubMed: 24737920]
21. Liu G, Chen Z. Phase-Resolved Doppler Optical Coherence Tomography. Selected Topics in Optical Coherence Tomography. 2012 InTech, Available: http://www.intechopen.com/books/selected-topics-in-optical-coherence-tomography/phase-resolveddoppler-optical-coherence-tomography.
22. Lackner B, Schmidinger G, Pieh S, Funovics MA, Skotpik C. Repeatability and Reproducibility of Central Corneal Thickness Measurement With Pentacam, Orbscan, and Ultrasound. Optometry and Vision Science. 2005; 82(10):892–899. [PubMed: 16276321]
23. Denoyer A, Ossant F, Arbeille B, Fetissof F, Patat F, Pourcelot L, Pisella PJ. Very-High-Frequency Ultrasound Corneal Imaging as a New Tool for Early Diagnosis of Ocular Surface Toxicity in Rabbits Treated with a Preserved Glaucoma Drug. Ophthalmic Research. 2008; 40(6):298–308. [PubMed: 18506111]

Biographies

Yueqiao Qu received the B.S. degree in biomedical engineering from the Johns Hopkins University in 2011 and the M.S. degree in biomedical engineering from the University of California, Irvine in 2015. She is currently a Ph.D. candidate working under the guidance of Dr. Z. Chen. In 2014, She was awarded the Cardiovascular Applied Research and Entrepreneurship Fellowship, offered by the Edwards Lifesciences Center for Advanced Cardiovascular Technology and the National Institutes of Health T32 grant. Her research interests include ARF-OCE technology development and applications in ophthalmology and cardiology, integrated intravascular ultrasound (IVUS) and OCT imaging, and miniature optical fiber catheter development for photoacoustic imaging, IVUS-OCT, and ARF-OCE.

Teng Ma received his B.S.E degree from University of Michigan, Ann Arbor, USA majoring in Biomedical Engineering in 2011. He received his M.S. degree and Ph.D degree in Biomedical Engineering from University of Southern California, Los Angeles, USA in 2013 and 2015. He joined NIH Resource Center for Medical Ultrasonic Transducer Technology as a Research Assistant and Ph.D. candidate under supervision of Dr. K. Kirk Shung and Dr. Qifa Zhou. In 2013, two of his papers were selected as “Best Student Paper Finalist” and featured in the 2013 Joint UFFC, EFTF and PFM Symposium. His research interests include medical ultrasound technology and multi-modality intravascular imaging by combining ultrasonic and optical techniques, such as intravascular ultrasound (IVUS), intravascular optical coherence tomography (IV-OCT), intravascular photoacoustic imaging (IVPA), and acoustic radiation force optical coherence elastography (ARF-OCE). He is also actively working in translational research and medical device commercialization with entrepreneurial spirit to translate innovative technology from research to clinical benefits.

Youmin He received the B.S and M.S degree in the School of Electronics and Information Engineering from Beijing Jiaotong University in 2011 and 2014, respectively. He is now a visiting scholar working in the group of Dr. Z.Chen. His research interests include fast OCT imaging algorithms and ARF-OCE technology development.

Jiang Zhu received the Ph.D. degree in biology from Tsinghua University in 2009. He is now a postdoctoral researcher in Beckman Laser Institute. His interests include optical coherence elastography and Doppler OCT.

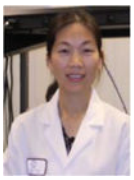

Cuixia Dai received her Ph. D. degree in Optical Engineering from Shanghai Institute of Optics and Fine Mechanics, Chinese Academy of Sciences in 2006. And she joined in School of Mechtronics Engineering and Automation Shanghai University in the same year. She is currently working in Shanghai Institute of Technology as an Associate Professor. Her research interest are on ophthalmology, optical coherence tomography and multimodality imaging.

Mingyue Yu was born in Hebei Province, China. She received a B.E. degree from Tianjin University, China in 2009. She started her Ph.D. study at University of Southern California (USC), Los Angeles, California in 2013 under the support of the USC Provost's Fellowship. Under the instruction of Dr. Qifa Zhou and Dr. K. Kirk Shung, Mingyue is conducting her research in the NIH Ultrasonic Transducer Resource Center (UTRC) on high-frequency ultrasonic transducer technology and intravascular ultrasonic imaging.

Shenghai Huang is now a PhD student in the Ocular Imaging Laboratory, Wenzhou Medical University. He is focusing on the application of optical coherence tomography (OCT) in ophthalmology and mainly involved in the development of functional OCT systems and image processing for retina in OCT images. In 2014, he was a visiting research scholar in Dr. Zhongping Chen's group at the Beckman Laser Institute, University of California for developing a Doppler OCT system in ophthalmology.

Fan Lu is a professor of ophthalmology and optometry. She is the president of Wenzhou Medical University (WZMU) and director of the Eye Hospital, WZMU. Her research focuses on the development and mechanism of myopia. She is a committee member of the Chinese Ophthalmology Society and secretary of the China National Optometry Research Center.

K. Kirk Shung obtained a B.S. degree in electrical engineering from Cheng-Kung University in Taiwan in 1968; an M.S. degree in electrical engineering from the University of Missouri, Columbia, MO, in 1970; and a Ph.D. degree in electrical engineering from the University of Washington, Seattle, WA, in 1975. He taught at The Pennsylvania State

University, University Park, PA, for 23 years before moving to the Department of Biomedical Engineering, University of Southern California, Los Angeles, *CA*, as a professor in 2002. He is the Dean's professor at University of Southern California. He has been the director of the NIH Resource on Medical Ultrasonic Transducer Technology since 1997. Dr. Shung is a life fellow of IEEE and a fellow of the Acoustical Society of America and the American Institute of Ultrasound in Medicine. He is a founding fellow of the American Institute of Medical and Biological Engineering. He received the IEEE Engineering in Medicine and Biology Society Early Career Award in 1985 and was the coauthor of a paper that received the best paper award for the *IEEE Transactions on Ultrasonics, Ferroelectrics, and Frequency Control* (UFFC) in 2000. He was elected an outstanding alumnus of Cheng-Kung University in Taiwan in 2001. He was selected as the distinguished lecturer for the IEEE UFFC society for 2002–2003. He received the Holmes Pioneer Award in Basic Science from the American Institute of Ultrasound in Medicine in 2010. He was selected to receive the academic career achievement award from the IEEE Engineering in Medicine and Biology Society in 2011. Dr. Shung has published more than 400 papers and book chapters. He is the author of the textbook *Principles of Medical Imaging*, published by Academic Press in 1992 and the textbook *Diagnostic Ultrasound: Imaging and Blood Flow Measurements*, published by CRC Press in 2005. He co-edited the book *Ultrasonic Scattering by Biological Tissues*, published by CRC Press in 1993. He is an associate editor of the *IEEE Transactions on Ultrasonics, Ferroelectrics, and Frequency Control* and a member of the editorial board of *Ultrasound in Medicine and Biology*. Dr. Shung's research interests are in ultrasonic transducers, high-frequency ultrasonic imaging, ultrasound microbeams, and ultrasonic scattering in tissues.

Qifa Zhou received his Ph. D. degree from the Department of Electronic Materials and Engineering of Xi'an Jiaotong University, China in 1993. He is currently a Research Professor at the NIH Resource on Medical Ultrasonic Transducer Technology and the Department of Biomedical Engineering and Industry & System Engineering at the University of Southern California (USC), Los Angeles, *CA*. Before joining USC in 2002, he worked in the Department of Physics at Zhongshan University in China, the Department of Applied Physics, Hong Kong Polytechnic University, and the Materials Research Laboratory, Pennsylvania State University. Dr. Zhou is a fellow of International Society for Optics and Photonics (SPIE) and American Institute for Medical and Biological Engineering (AIMBE).He is also a senior member of the IEEE Ultrasonics, Ferroelectrics, and Frequency Control (UFFC) Society and a member of the UFFC Society's Ferroelectric Committee. He is a member of the Technical Program Committee of the IEEE International Ultrasonics Symposium. He is an Associate Editor of the *IEEE Transactions on Ultrasonics, Ferroelectrics, and Frequency Control*. His current research interests include the development of ferroelectric thin films, MEMS technology, nano-composites, and modeling and fabrication of high-frequency ultrasound transducers and arrays for medical imaging

applications, such as photoacoustic imaging and intravascular imaging. He has published more than 130 journal papers in this area.

Zhongping Chen received the B.S. degree in applied physics from Shanghai Jiao Tong University, Shanghai, China, in 1982, the M.S. degree in electrical engineering from Cornell University, NY, USA, in 1987, and the Ph.D. degree in applied physics from Cornell University in 1993. He is currently a Professor of biomedical engineering and the Director of F-OCT Laboratory at the University of California, Irvine, CA, USA. He is a cofounder and the Board Chairman of OCT Medical Imaging, Inc. His research interests encompass the areas of biomedical photonics, microfabrication, biomaterials, and biosensors. His research group has pioneered the development of functional optical coherence tomography, which simultaneously provides high-resolution 3-D images of tissue structure, blood flow, and birefringence. He has published more than 220 peer-reviewed papers and review articles and holds a number of patents in the fields of biomaterials, biosensors, and biomedical imaging. Dr. Chen is a Fellow of the American Institute of Medical and Biological Engineering (AIMBE), a Fellow of SPIE, and a Fellow of the Optical Society of America.

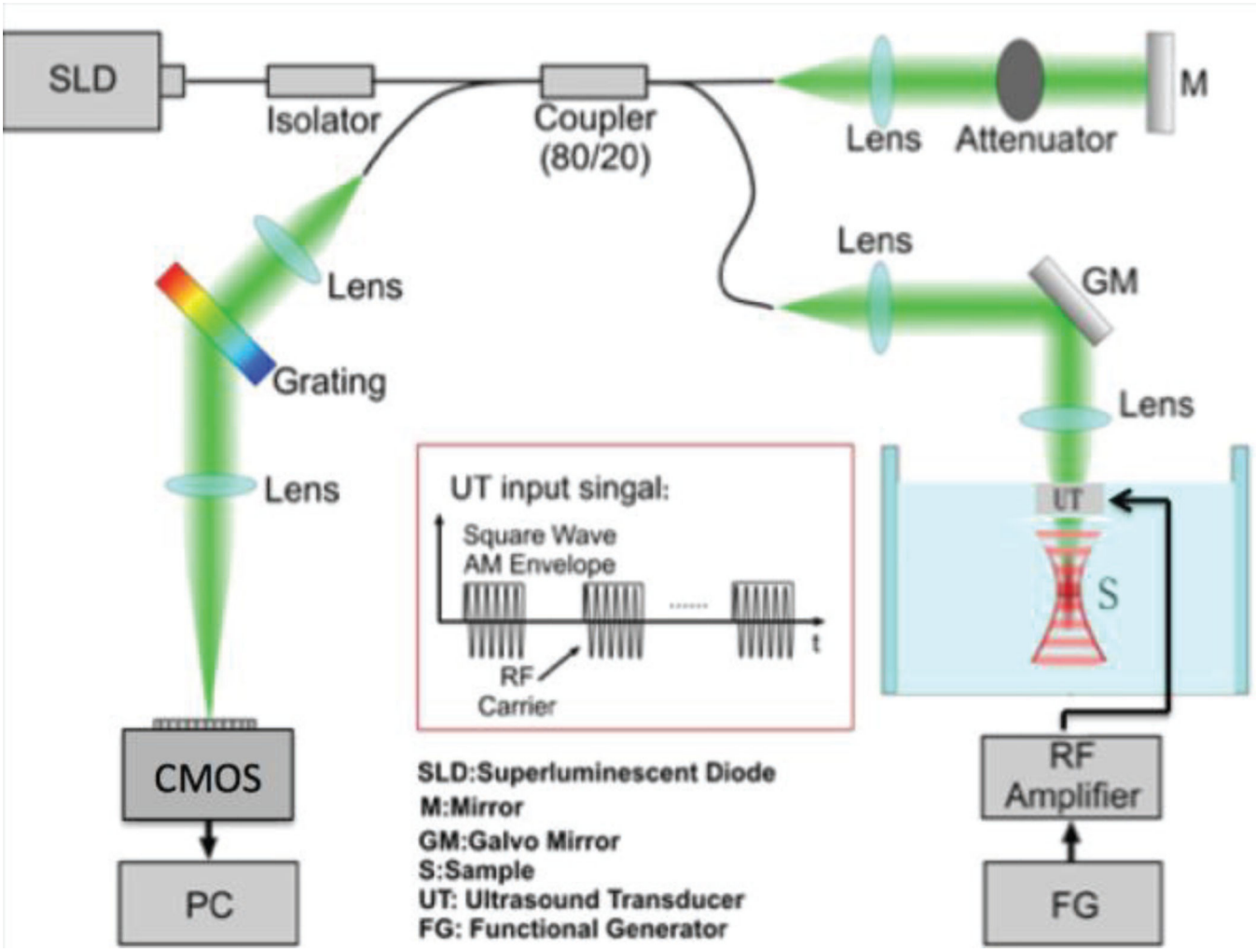

Fig. 1.
Schematic diagram of OCE system. RF: radiofrequency, CMOS: camera.

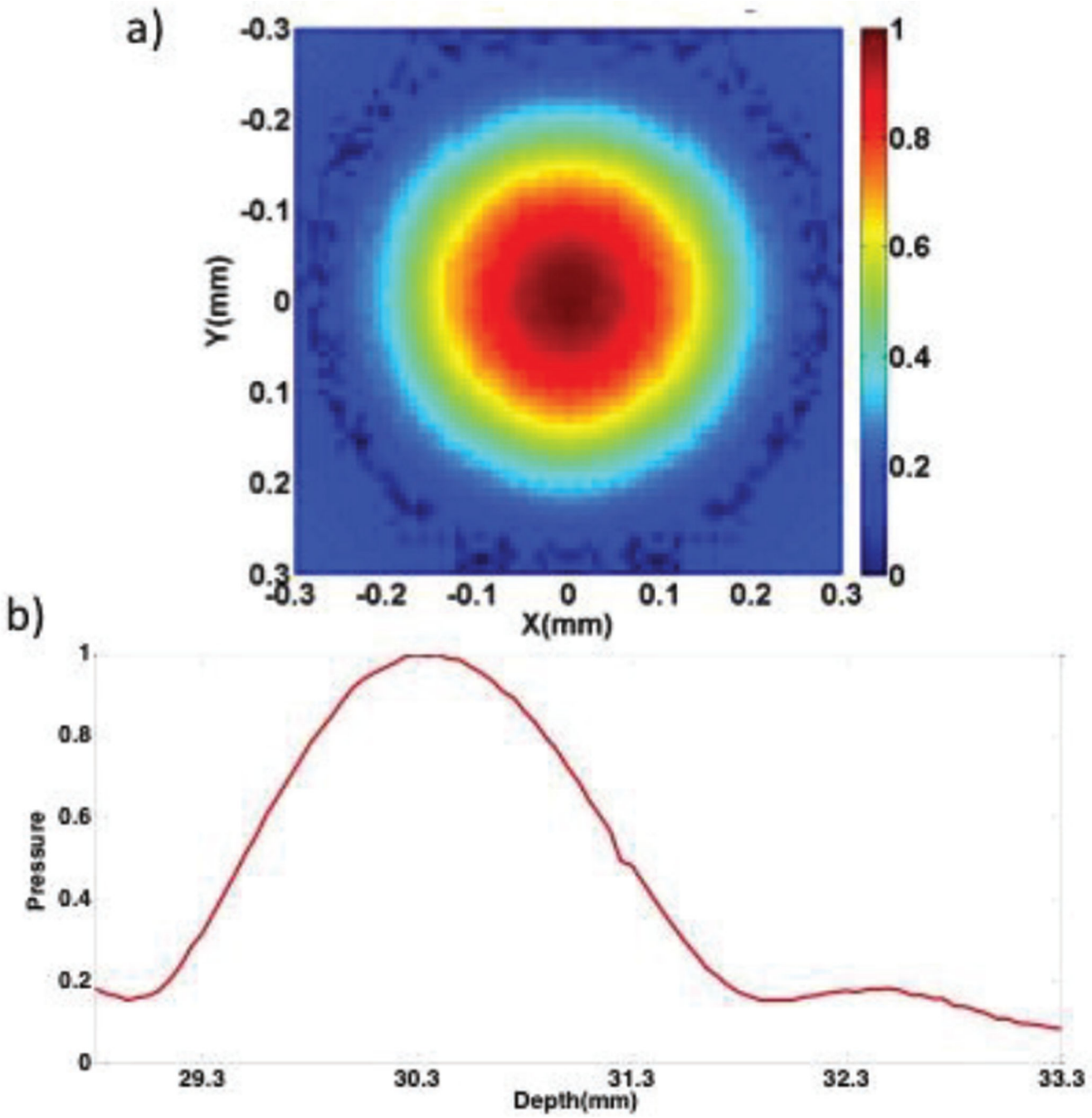

Fig. 2.

Ring Transducer Beam Profile. a. Normalized pressure profile at the axial focus. b. Normalized axial beam profile.

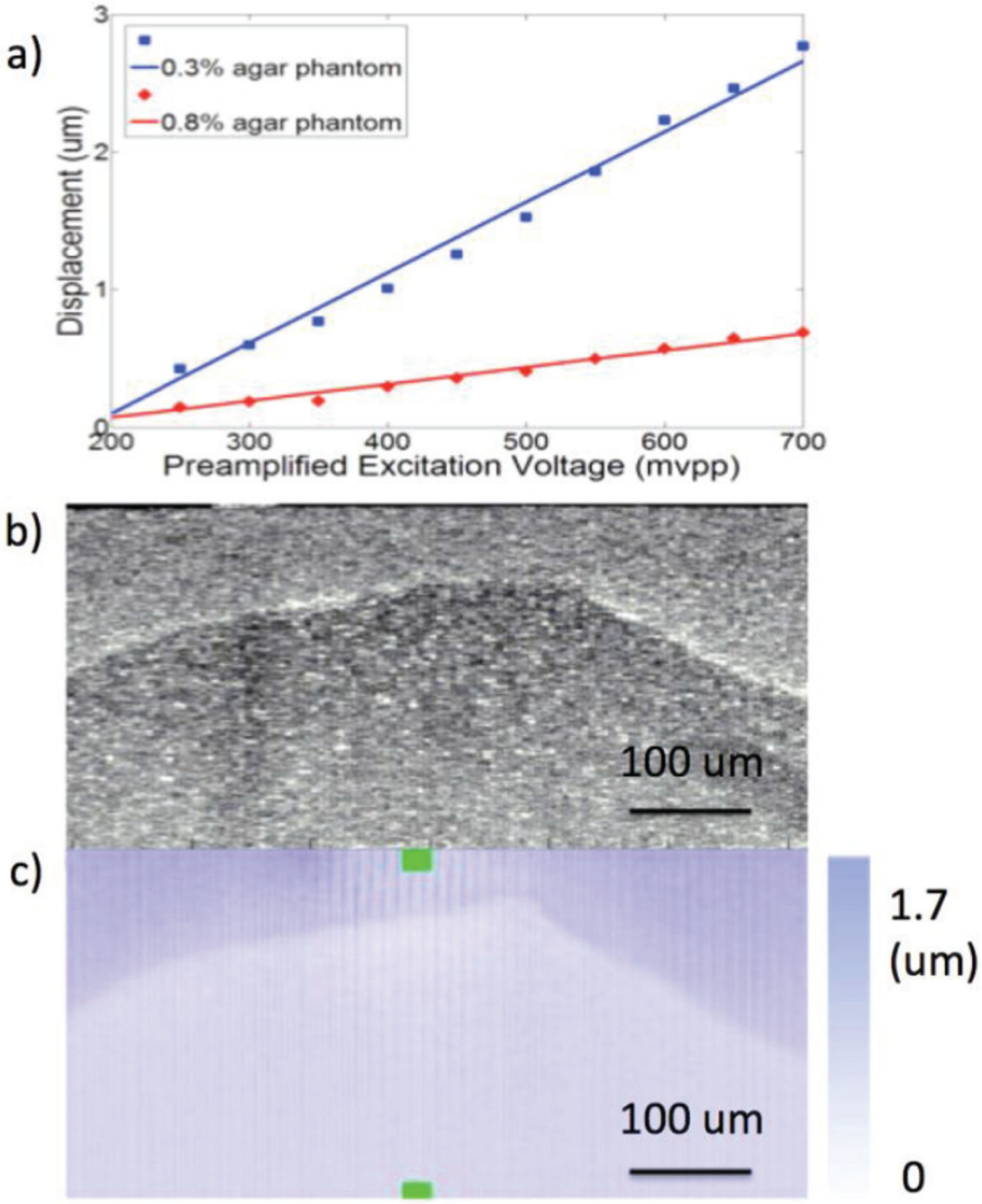

Fig. 3.

Phantom testing. a. Displacement under different excitation voltages for two phantoms of different stiffness. b. OCT image of inclusion phantom. c. OCE projection image of inclusion phantom.

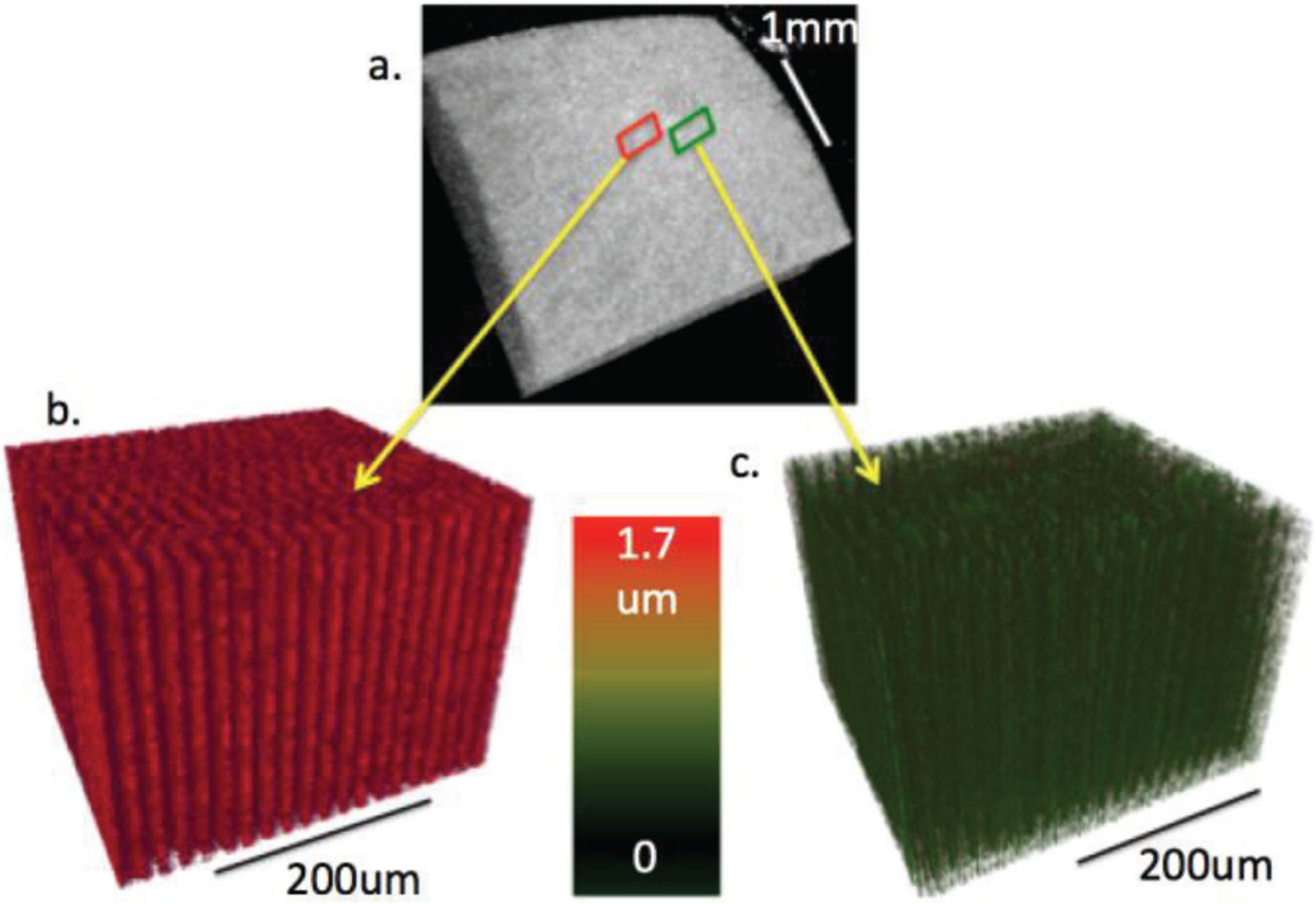

Fig. 4.

3-D images of rabbit cornea with and without formalin crosslinking. a. 3-D OCT reconstruction of 3 mm by 3 mm section of cornea. b. 3-D OCE section of healthy cornea. c. 3-D OCE section of cross-linked cornea.

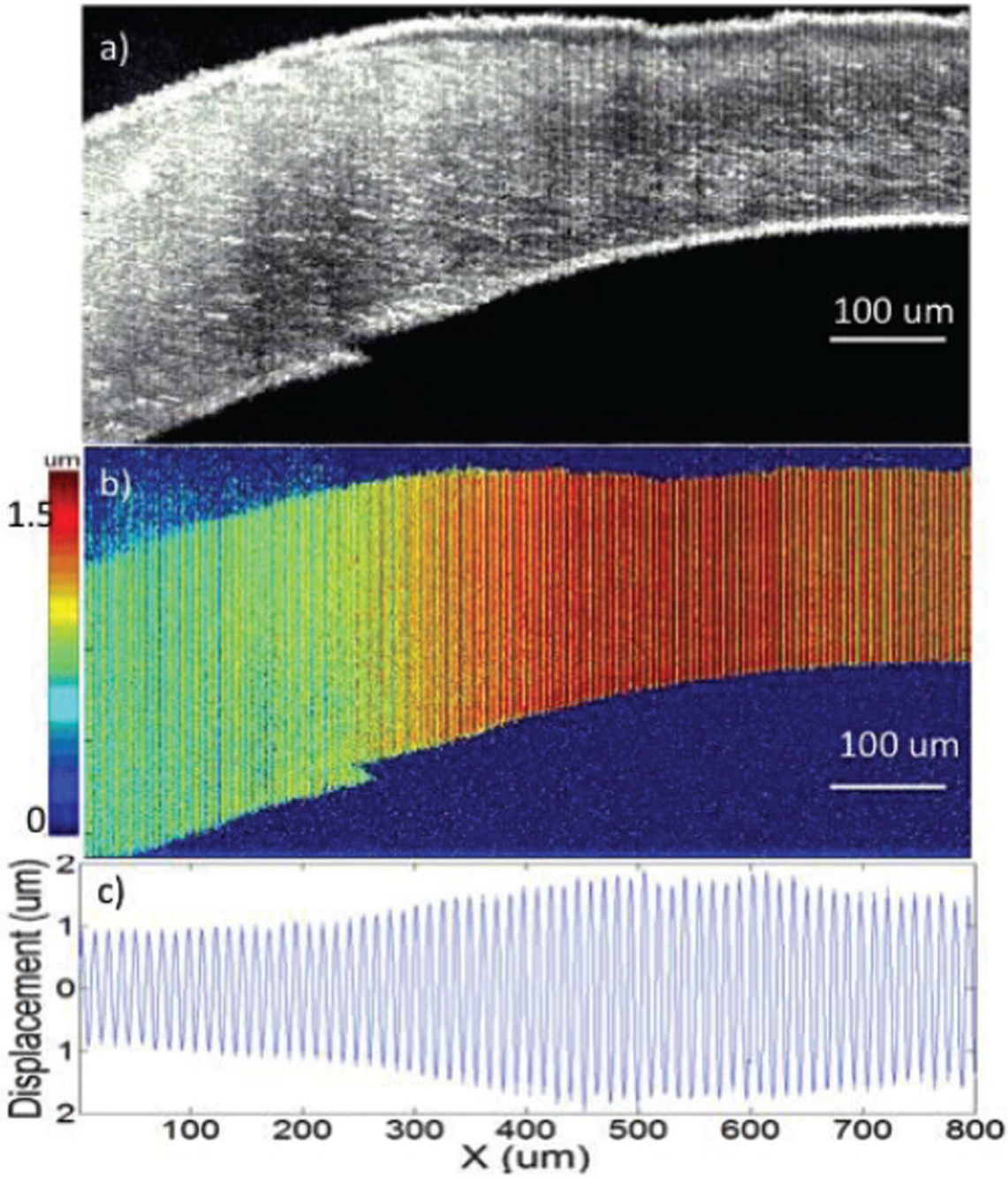

Fig. 5.

Imaging of rabbit cornea with injection of formalin solution. a. OCT image of cornea. b. OCE displacement magnitude image of cornea. c. Quantified displacement of cornea.